A DUAL-USE BALLUTE FOR ENTRY AND DESCENT DURING PLANETARY MISSIONS

Kristin L. (Gates) Medlock[1], James M. Longuski[2], Daniel T. Lyons[3]

[1] Graduate Student, Purdue University, Aeronautics & Astronautics, West Lafayette, IN 47907-2023, USA
Email: gatesk@purdue.edu
[2] Professor, Purdue University, Aeronautics & Astronautics, West Lafayette, IN 47907-2023, USA
Email: longuski@ecn.purdue.edu
[3] Senior Engineer, Jet Propulsion Laboratory, California Institute of Technology, Pasadena, CA 91109-8099, USA
Email: daniel.t.lyons@jpl.nasa.gov

ABSTRACT

An inflatable ballute system for aerocapture at the atmosphere-bearing planets and at Titan may provide significant performance benefits, compared to conventional propulsive capture and aerocapture technologies. Ballute simulations to date release the ballute at the appropriate instant and then ignore it to focus on the trajectory of the orbiter. The latest concept, which we pursue in this paper, is to employ the ballute to soft-land a small payload. Thus the same ballute can provide two uses (1) aerocapture of the orbiter and (2) soft-landing of the lander package, hence the term dual-use ballute. The dual-use ballute concept has the potential to dramatically alter the way we approach exploration of the atmosphere-bearing bodies in the Solar System. Cases investigated here include aerocapture and soft-landing at Mars, Titan and Neptune.

1. INTRODUCTION

The ballute (a term originating from balloon-parachute) provides a large aerodynamic drag area to achieve orbit insertion. The ballute's large area-to-mass ratio allows the vehicle to stay high in the atmosphere where the heating rate is lower.

Traditional propulsive capture is not cost effective, in that it requires the vehicle to carry large amounts of propellant for insertion into low altitude orbits. The small reference areas associated with aerocapture using a lifting-body (or aeroshell) requires the spacecraft to dive deep into the atmosphere where the densities are higher. The high densities result in high heating rates and necessitate additional mass for heat shielding. The use of a large, lightweight inflatable device for aerocapture could provide a significant mass savings over the previously mentioned capture vehicles.

During ballute aerocapture, the orbiter approaches the planetary body on a hyperbolic trajectory, deploying the ballute before entering the atmosphere. Inside the atmosphere, the vehicle begins to decelerate at a rapidly increasing rate. Once the desired velocity change is achieved, the ballute is released allowing the orbiter to exit the atmosphere, where it can propulsively raise periapsis and achieve the desired orbit.

If a lander package remains attached to the ballute, it will inevitably land on the surface enabling the ballute to provide dual-function, as depicted in Fig. 1.

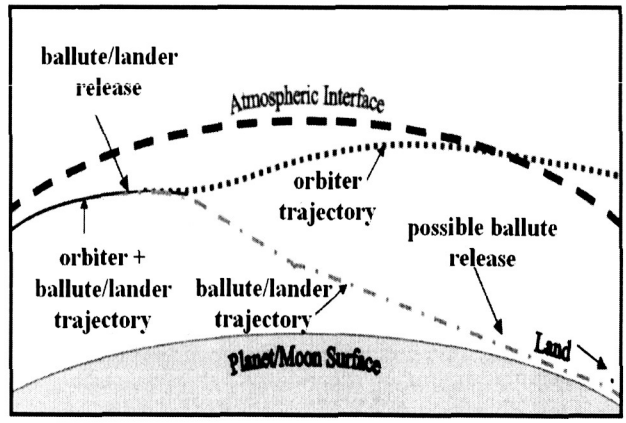

Fig. 1. Dual-Use Ballute Schematic

In this paper, we explore the feasibility of a dual-use ballute through specific trajectory simulations generated by Global Aerospace Corporation's HyperPASS simulation software [1]. Trajectory simulations are conducted for aerocapture and soft-landing at Mars, Titan and Neptune, as representative cases.

2. BACKGROUND

Because of performance advantages and mass savings potential, a significant amount of research has been carried out to investigate the feasibility of different ballute systems and missions. A systems level study of ballutes for aerocapture at several planetary bodies has been conducted by McRonald [2-4] and an extensive review of ballute technology is provided by Hall [5]. K. Miller et al. [6] characterize and refine the use of ballutes for future aerocapture missions. Current research is ongoing at a number of companies and laboratories including Ball Aerospace, ILC Dover, NASA Langley Research Center, and The Jet Propulsion Laboratory. In addition, Lyons and McRonald [7] have recently done some preliminary studies on the feasibility of using a dual-use ballute system at Titan.

Fig. 2 illustrates one possible configuration (a tethered toroid, commonly called a towed ballute). Another configuration is the clamped ballute (where a ballute is directly attached to the spacecraft without the use of tethers). Variations on these basic ideas are also being considered.

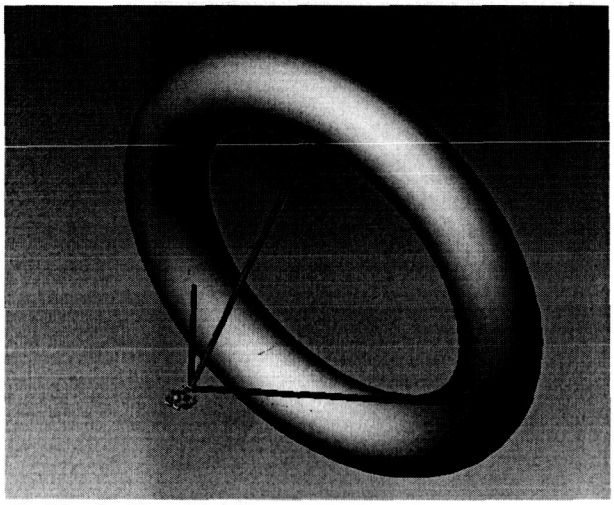

Fig. 2. Toroidal Towed Ballute Configuration (from Lyons and McRonald [7])

3. ISSUES

Making aerocapture and landing with a ballute a reality is a formidable task for a host of reasons that have been identified by numerous investigators [5, 6]. In the interest of brevity, we merely provide the following list with key references:

1. Determination of the optimal ballute shape and configuration [6, 8],
2. Heating and material limits [9, 10],
3. Packing and storage [5],
4. Trajectory robustness [12-15],
5. Flow stability [16-21],
6. Aeroelasticity [22],
7. Deployment and inflation [23], and
8. Tether design for towed ballutes [6].

If these technological challenges are surmountable, then the dual-use concept will be feasible for aerospace applications. While several of these issues have been described in detail by the authors referenced, we will assume all of the issues have been resolved for the purpose of our study. We now take a look at trajectory simulations and numerical analysis for our three reference cases.

4. NUMERICAL RESULTS

To demonstrate the dual-use ballute concept, trajectory simulations are conducted at Mars, Titan and Neptune using HyperPASS [1]. Some features of HyperPASS include the capability to perform guided aerocapture, guided ballute aerocapture, aerobraking, and unguided user-entered trajectory simulations. In order to perform the dual-use ballute simulations, we modified the HyperPASS code to include simulation for descent to the surface. HyperPASS incorporates the following assumptions for trajectory propagation and calculations:

- Spherical planetary body
- Inverse-square gravity field
- Rotating atmosphere (with planet)
- Point-mass vehicle representation
- Exponentially interpolated atmosphere
- Constant drag coefficient (C_D) model

The Mars, Titan and Neptune cases presented here use the same orbiter+ballute/lander sysem (described in Table 1) for the purpose of comparison. Since these parameters were developed for a Titan example, they may not work at Neptune, where the entry speeds are significantly higher. Simulation parameters at Titan and Neptune are adapted from previous studies [6, 12-15] and are displayed in Table 2; the target apoapsis at Mars is chosen to achieve a 7-day parking orbit. HyperPASS chooses an entry flight path angle (FPA) by selecting the steepest entry that allows the orbiter to barely exit the atmosphere (assuming the ballute is not released). Thus, the chosen exit orbit will be nearly circular. Because the target apoapsis altitude is higher than that of the chosen exit orbit, it is guaranteed that the ballute

will be released inside the atmosphere. The trajectory is then propagated, releasing the ballute at the appropriate time to achieve the target exit conditions (corresponding to an eccentric orbit).This method allows the vehicle to dive deep enough to accommodate navigation and atmospheric uncertainties while still maintaining a high enough trajectory to keep the heating rates low. (These uncertainties are not modeled in the present code and our current approach may not provide the lowest possible heating rates.)

Table 1 Vehicle Parameters for Dual-Use Ballute Simulations at Mars, Titan and Neptune

Parameter	Orbiter	Ballute/Lander
m	400 kg	100 kg
C_D	1.37	1.37
A	2 m^2	750 m^2
R_n	0.8 m	15.5 m

Table 2 Entry and Target Conditions for Dual-Use Ballute Simulations at Mars, Titan and Neptune

Condition	Mars	Titan	Neptune
Entry/Exit Altitude, km	150	1025	1500
Inertial Entry Speed, km/s	5.75	6.5	23.6
Inertial Entry FPA, deg	-8.49	-30.50	-11.10
Target Apoapsis Altitude, km	16685	1700	430,000

Fig. 3 shows the time history of the altitude during the atmospheric flight of each trajectory. The entry altitudes and release times are depicted by dashed lines labeled on the plots (we note that all of the release times occur within 10 minutes of entry). The orbiter altitude is decreasing while the ballute is attached. Because the nominal trajectory is targeted low enough to accommodate uncertainties, the ballute is released before periapsis is reached in each example. The orbiter has enough speed to escape the atmosphere (indicated by a U-shaped trajectory), while the ballute and anything still attached to it will always end up on the surface (indicated by asymptotic descent to zero altitude).

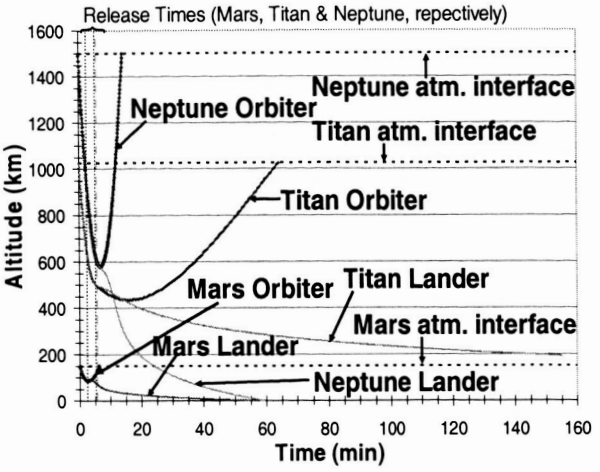

Fig. 3. Altitude vs. Time Since Entry

Fig. 4 shows the velocity history during atmospheric flight. Initially, velocity relative to the atmosphere decreases rapidly from drag acting on the ballute. After release, the orbiter speed decreases as altitude increases, while the ballute/lander speed decreases rapidly until terminal velocity is achieved. Slow speed relative to the atmosphere means that winds will perturb the landing site which is not desirable for precision landing. The perturbation may be alleviated by releasing the ballute before landing. An alternate scheme is to employ a steerable parachute.

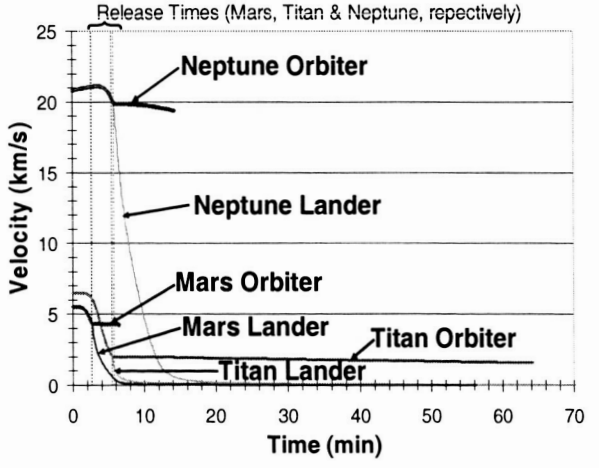

Fig. 4. Velocity vs. Time Since Entry

Prior to running the simulations, we calculated the terminal velocity (v_{term}) for each case,

$$v_{term} = \left(\frac{2mg_{planet}}{\rho_o C_D A} \right)^{1/2} \quad (1)$$

where m and A are the mass and reference area of the ballute/lander (sans orbiter), respectively. Table 3 shows the results of this calculation, as well as other planet-specific parameters including gravitational constant (g_{planet}), reference atmospheric density (ρ_o), and planet radius (R_{planet}). In the case of Neptune, we define the "surface" at an atmospheric density of 0.0013 kg/m^3 which corresponds to a radius of 24764 km. Fig. 5 shows the approach to terminal velocity for the ballute/lander at each target body, referenced to the defined planetary surface. In all three cases, near the end of the trajectory, the ballute/lander descends at (very nearly) the instantaneous terminal velocity (until it slows to the surface terminal velocity indicated in Fig. 5).

Table 3 Terminal Velocity Calculation at Titan, Mars, and Neptune

	Titan	Mars	Neptune
g_{planet}	1.3541 m/s^2	3.7114 m/s^2	11.1456 m/s^2
ρ_o	5.68 kg/m^3	0.0155 kg/m^3	0.0013 kg/m^3
R_{planet}	2575 km	3397 km	24764 km
v_{term}	0.215 m/s	6.83 m/s	40.85 m/s

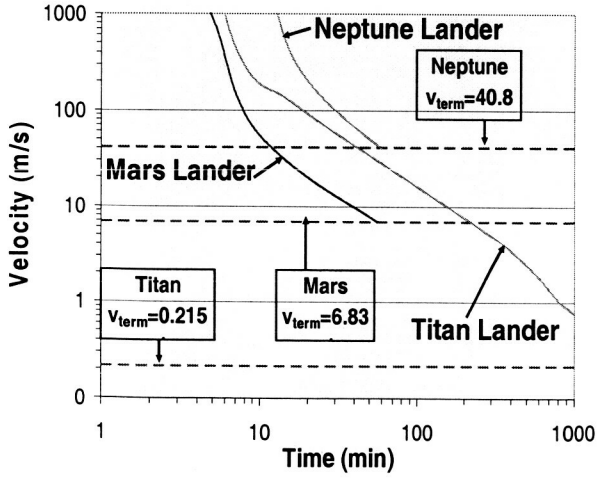

Fig. 5: Approach to Terminal Velocity vs. Time (logarithmic scale) Since Entry

The ballute release times presented here are selected by HyperPASS to hit the orbiter target condition exactly. In applications, an onboard separation algorithm will be used to estimate the drag effect on the orbiter after separation in order to release the ballute at the appropriate time. Propellant will be required to raise the periapsis of the orbiter out of the atmosphere and up to the target orbit altitude. Additional propellant will be needed to adjust the apoapsis altitude if the ballute is released too early or too late.

In Fig. 6 we see that upon entering the atmosphere, the large drag area causes rapid deceleration that can reach several Earth G's. Ballute release occurs after the maximum deceleration, so deceleration on the orbiter drops suddenly at release and remains low even though the dynamic pressure is largest near periapsis, as shown in Fig. 7. On the contrary, the deceleration of the ballute/lander increases suddenly since the force remains large, but the mass becomes small. Therefore, the lander hardware will have to be designed to accommodate a higher G-load than the orbiter (the lighter the lander package, the higher the G-load).

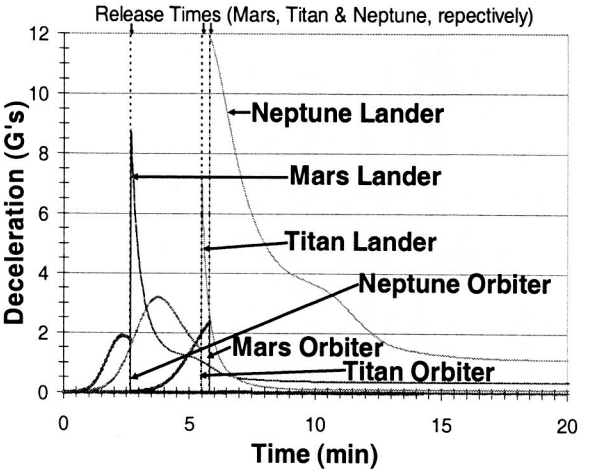

Fig. 6. Deceleration vs. Time Since Entry

In Fig. 7 dynamic pressure is calculated by:

$$P_{dyn} = \frac{1}{2}\rho v^2 \qquad (2)$$

The dynamic pressure determines the inflation pressure required to maintain the shape of the ballute during capture; it is also used to compute aeroelastic effects and tether loads [6].

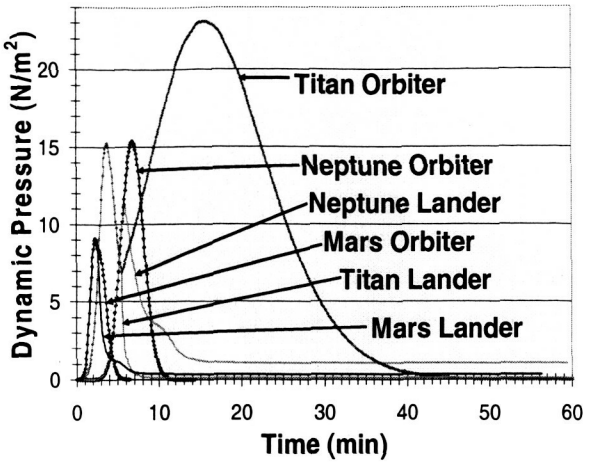

Fig. 7. Dynamic Pressure vs. Time Since Entry

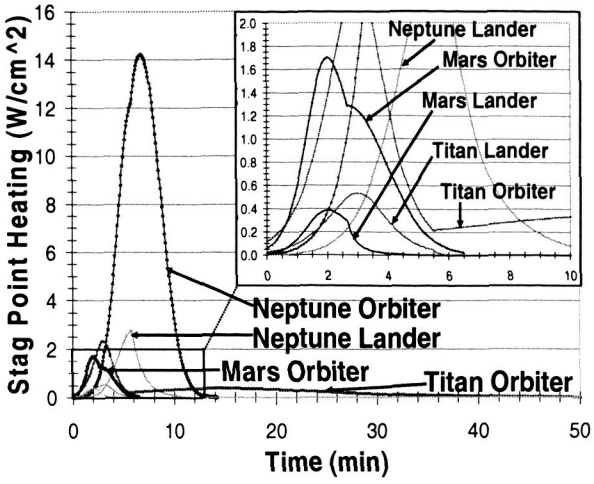

Fig. 8. Stagnation-Point Heating vs. Time Since Entry

One of the more promising of the candidate ballute materials currently being investigated is Kapton. A heating limit of 3 W/cm^2 is applied to this study based on Kapton's rated temperature of 500°C [6]. Figure 8 shows the stagnation-point heating during atmospheric flight calculated using,

$$Q_{stag} = \frac{C\rho^{Nstag} v^{Mstag}}{\sqrt{R_n}} \qquad (3)$$

which is similar to the Sutton-Graves convective heating equation [24]. In Eq. 3, ρ is atmospheric density, v is planet relative velocity, R_n is the nose radius of the vehicle, *Nstag* and *Mstag* are the density and velocity coefficients (typical values of Nstag = 0.5 and Mstag = 3.05 are used for this study), and C is the stagnation point heating coefficient. The stagnation-point heating coefficient (C) varies according to the planet. We use 9.80 x 10^{-5}, 9.00 x $10^{-5}$and 3.54 x 10^{-5} kg$^{0.5}$/m for Mars, Titan and Neptune, respectively. The R_n of the ballute/lander is calculated assuming a spherical ballute. In Fig. 8 we see that the stagnation-point heating rate is much higher for the orbiter than for the ballute/lander in each of the reference cases. This divergence is due to the large difference in R_n (0.80 m^2 for the orbiter and 15.5 m^2 for the ballute/lander). The cases at Mars and Titan stay within the maximum heating limit of 3 W/cm^2. In the case at Neptune, the stagnation-point heating on the orbiter exceeds 14 W/cm^2, while the heating on the ballute/lander remains below 3 W/cm^2. Thus the Neptune mission will require a smaller orbiter mass, or a larger ballute area, or additional shielding than missions to Mars or Titan.

When considering aerocapture with a towed ballute configuration, at least 3 different heating rates are needed because there are three different characteristic sizes associated with the tether, ballute and spacecraft. The free stream heat flux:

$$Q_{fm} = \frac{1}{2}\rho v^3 \qquad (4)$$

is appropriate for nearly free molecular flow, which is the case for the thin tethers used to connect the large inflated towed ballute to the lander and orbiter. Free molecular flow is representative when the most of the atmospheric molecules are likely to hit the spacecraft without interacting with molecules that have already transferred their energy and momentum to the spacecraft. The fraction of Q that is transferred to heat the spacecraft is higher for free molecular flow, because individual molecules can hit the spacecraft at full orbital speed. Although the inflated ballute is flying through the same atmosphere as the rest of the spacecraft, the ballute is orders of magnitude larger than the tether, and can reach conditions that are best characterized by continuum flow (or stagnation-point heating) approximations where the heating is proportional to the square root of the density rather than the density itself, as shown in Eq. 3. The characteristic size of the spacecraft is in between these extremes, and so is the heating rate [12].

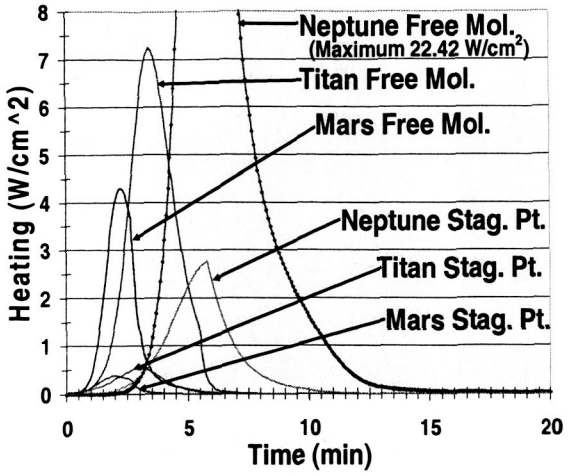

Fig. 9. Free Molecular and Stagnation-Point Heating Comparison

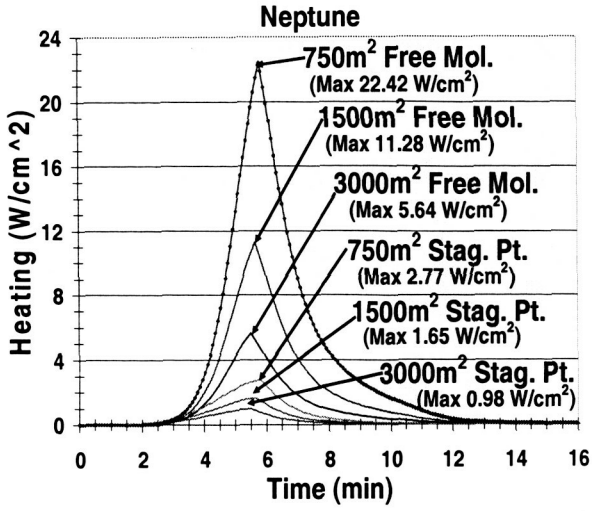

Fig. 10. Heating Comparison for a 750m², 1550m² and 3000m² Ballute at Neptune

Fig. 9 shows a comparison of the free molecular heating rate and stagnation-point heating calculation for the ballute system (orbiter+ballute/lander prior to separation and ballute/lander only after separation). The free molecular heating rates are higher than the stagnation point heating rates at each target body. While the free molecular heating for the cases at Mars and Titan also exceed the maximum heating rate (7.2 W/cm^2 and 4.3 W/cm^2, respectively) we note that the stagnation-point heating is far below the maximum of 3 W/cm^2. As mentioned previously, the heating rates at Neptune exceed the material limit of the ballute, so a 750 m^2 ballute is not feasible. Fig. 10 shows the heating result of a ballute sizing study done at Neptune by varying only the ballute's reference area (750 m^2, 1500 m^2, and 3000 m^2). The R_n for each case is again calculated assuming a spherical ballute with the given reference area (i.e. 15.5 m^2, 21.9 m^2, and 30.9 m^2, respectively). The maximum free molecular heating rate is nearly cut in half by doubling the ballute area. It is probable that the heating problem at Neptune could be resolved if larger area-to-mass ratios are proven feasible. Simulations with a 1500 m^2 ballute were also conducted at Mars and Titan. The resulting peak free molecular heating rates (1.99 W/cm^2 and 2.90 W/cm^2, respectively) fall within the 3 W/cm^2 constraint.

5. CONCLUSIONS

If the aforementioned technical issues can be surmounted, the dual-use ballute offers tremendous advantages for exploration of atmosphere-bearing bodies in the Solar System. The dual-use ballute is particularly efficient in delivering payloads to the surfaces of Titan and Mars. We would also expect excellent applications at Venus and perhaps for Earth return missions. For the distant gas giant Neptune, a dual-use ballute must be designed to increase the area-to-mass ratio above current practical limits to accommodate the heating rate. Overall the dual-use ballute offers a significant new technique for the exploration of the Solar System.

6. ACKNOWLEDGEMENTS

Part of the work described in this paper was performed at Purdue University under contract with National Aeronautics and Space Administration (NASA). Funding for this study was provided in part by Marshall Space Flight Center (MSFC), under Award No. NNM05AA22G. We would particularly like to thank Bonnie James at the MSFC In-Space Propulsion Program office for her sponsorship. Also, we would like to thank Mohammad Ayoubi (a doctoral candidate at Purdue University) for his assistance.

7. REFERENCES

1. Gates, K. L., McRonald, A. D., and Nock, K. T., "HyperPASS, a New Aeroassist Tool," 2nd International Planetary Probe Workshop, NASA Ames Research Center, Moffet Field, CA, Aug. 2004.

2. McRonald, A. D., "A Light-Weight Inflatable Hypersonic Drag Device for Planetary Entry," Association Aeronautique de France Conference, Arcachon, France, Mar. 16-18, 1999.

3. McRonald, A. D., "A Light-Weight Inflatable Hypersonic Drag Device for Venus Entry," AAS/AIAA Astrodynamics Specialist Conference, Girdwood, AK, AAS Paper 99-355, Aug. 16-19, 1999.

4. McRonald, A. D., "A Light-Weight Hypersonic Inflatable Drag Device for a Neptune Orbiter," AAS/AIAA Space Flight Mechanics Meeting, Clearwater, FL, AAS Paper 00-170, Jan. 23-26, 2000.

5. Hall, J. L., "A Review of Ballute Technology For Planetary Aerocapture," 4th IAA Conference on Low Cost Planetary Missions, Laurel, MD, May 2-5, 2000.

6. Miller, K. L., Gulick, D., Lewis, J., Trochman, B., Stein, J., Lyons, D. T., and Wilmoth, R. G., "Trailing Ballute Aerocapture: Concept and Feasibility Assessment," 39th AIAA/ASME/SAE/ ASEE Joint Propulsion Conference and Exhibit, Von Braun Center, Huntsville, AL, AIAA Paper 2003-4655, July 20-23, 2003.

7. Lyons, D. T. and McRonald, A. D., "Entry, Descent and Landing using Ballutes". Presentation at 2nd International Planetary Probe Workshop, NASA Ames Research Center, Moffet Field, CA, Aug. 2004.

8. Kustas, F. M., Rawal, S. P., Willcockson, W. H., Edquist, C. T., Thornton, J. M., and Sandy, C., "Inflatable Decelerator Ballute for Planetary Exploration Spacecraft," AIAA/ASME/ASCE/ AHS/ASC Structures, Structural Dynamics, and Materials Conference and Exhibit, 41st, Atlanta, GA, AIAA Paper 2000-1795, Apr. 3-6, 2000.

9. Xia, G., Cheng, W., and Qin, Z., "Development of Flexible Thermal Protection System for Inflatable Re-entry Vehicles," *Yuhang Cailiao Gongyi (Aerospace Materials and Technology)*, China, Vol. 33, No. 6, pp. 1-6, Nov.-Dec. 2003.

10. Kustas, F. M., Rawal, S. P., Willcockson, W. H., Edquist, C. T., Thornton, J. M., and Sandy, C., "Evaluation of High-temperature Multilayer Insulation for Inflatable Ballute," *Journal of Spacecraft and Rockets*, Vol. 38, No. 4, pp. 630, 631, July-Aug. 2001.

11. Finchenko V., Ivankov A., and Shmatov S. "Aerobraking and Aerocapture: Aerodynamic and Aerothermal Study, Applicability of Inflatable Structures," AIAA Aerodynamic Decelerator Systems Technology Conference and Seminar, 16th, Boston, MA, AIAA Paper 2001-2057, May 21-24, 2001.

12. Lyons, D. T. and Johnson, W. R., "Ballute Aerocapture Trajectories at Neptune," AIAA Atmospheric Flight Mechanics Conference and Exhibit, Providence, RI, AIAA Paper 2004-5181, Aug. 16-19, 2004.

13. Johnson, W. R. and Lyons, D. T., "Titan Ballute Aerocapture Using a Perturbed TitanGRAM Model," AIAA Atmospheric Flight Mechanics Conference and Exhibit, Providence, RI, AIAA Paper 2004-5280, Aug. 16-19, 2004.

14. Lyons, D. T. and Johnson, W. R., "Ballute Aerocapture Trajectories at Titan," *Advances in the Astronautical Sciences*, Vol. 116, Suppl. pp. 1-20, 2004.

15. Hall, J. L. and Le, A. K., "Aerocapture Trajectories for Spacecraft with Large, Towed Ballutes," 11th Annual AAS/AIAA Space Flight Mechanics Meeting, Santa Barbara, CA, AAS 01-235, Feb. 11-15, 2001.

16. Gnoffo, P. and Anderson, B., "Computational Analysis of Towed Ballute Interactions," 8th AIAA/ASME Joint Thermophysics and Heat Transfer Conference, Saint Louis, MO, AIAA Paper 2002-2997, June 24-26, 2002. .

17. Anderson, B. P., "Computational Continuum and Rarefied Flow Results for Ballute Applications," 42nd AIAA Aerospace Sciences Meeting and Exhibit, Reno, NV, AIAA Paper 2004-292, Jan. 5-8, 2004.

18. McIntyre, T. J., Lourel, I., Eichmann, T. N., Morgan, R. G., Jacobs, P. A., and Bishop, A I., "Experimental Expansion Tube Study of the Flow over a Toroidal Ballute," *Journal of Spacecraft and Rockets*, Vol. 41, No. 5, pp. 716-725, Sept.-Oct. 2004.

19. Hornung, H. G., "Hypersonic Flow Over Bodies in Tandem and its Relevance to Ballute Design," AIAA Fluid Dynamics Conference & Exhibit, 31st, Anaheim, CA, AIAA Paper 2001-2776, June 11-14, 2001.

20. Rasheed, A., Fujii, K., Hornung, H. G., and Hall, J. L., "Experimental Investigation of the Flow over a Toroidal Aerocapture Ballute," AIAA Applied Aerodynamics Conference, 19th, Anaheim, CA, AIAA Paper 2001-2460, June 11-14, 2001.

21. Park, C., "Theory of Idealized Two-Dimensional Ballute in Newtonian Hypersonic Flow," *Journal of Spacecraft and Rockets*, Vol. 25, No. 3, pp. 217-224, AIAA Paper 1986-301, May-June 1988.

22. Mosseev, Y., "The Decelerator Pitch-dependent Performances Prediction Based on 3D Aeroelastic Analysis," CEAS/AIAA Aerodynamic Decelerator Systems Technology Conference, 15th, Toulouse, France, AIAA Paper 1999-1717, June 8-11, 1999.

23. Westhelle, C. H. and Masciarelli, J. P., "Assessment of Aerocapture Flight at Titan Using a Drag-only Device," 2003 AIAA Atmospheric Flight Mechanics Conference and Exhibit, Austin, TX, AIAA Paper 2003-5389, Aug. 11-14, 2003.

24. Sutton, K. and Graves, R. A., Jr., "A General Stagnation Point Convective Heating Equation for Arbitrary Gas Mixtures," NASA TR R-376, NASA Langley Research Center, Hampton VA, Nov. 1971.

PURDUE
UNIVERSITY

A Dual-Use Ballute for Entry and Descent During Planetary Missions

Kristin L. (Gates) Medlock[1]
James M. Longuski[2]
Daniel T. Lyons[3]

3rd International Planetary Probe Workshop
Attica, Greece
June 27 - July 1, 2005

(1) Graduate Student, Purdue University
(2) Professor, Purdue University
(3) Senior Engineer, Jet Propulsion Laboratory

Funded by MSFC Award No. NNM05AA22G
(Bonnie F. James)

Dual-Use Ballute Concept

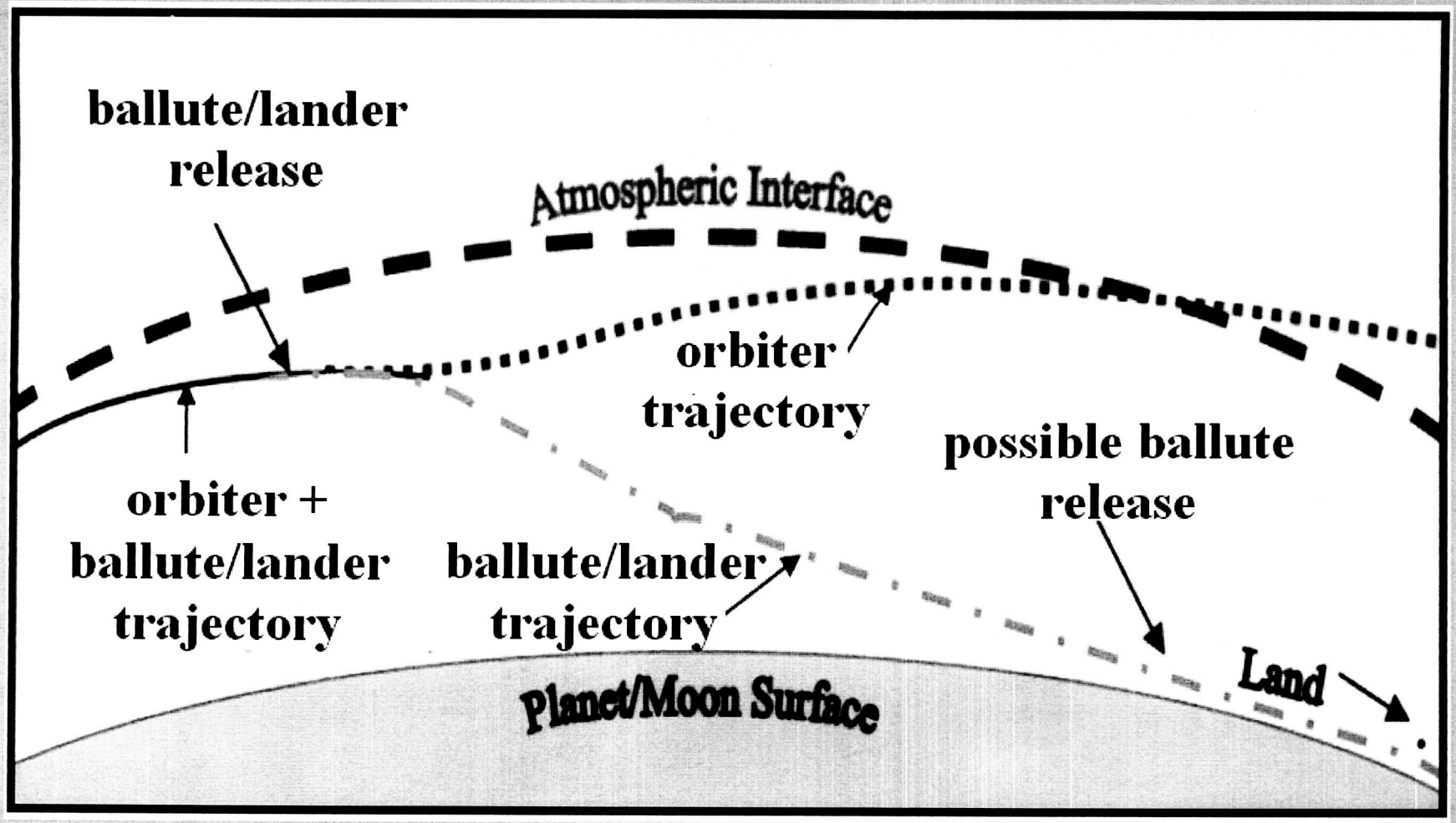

Technical Challenges

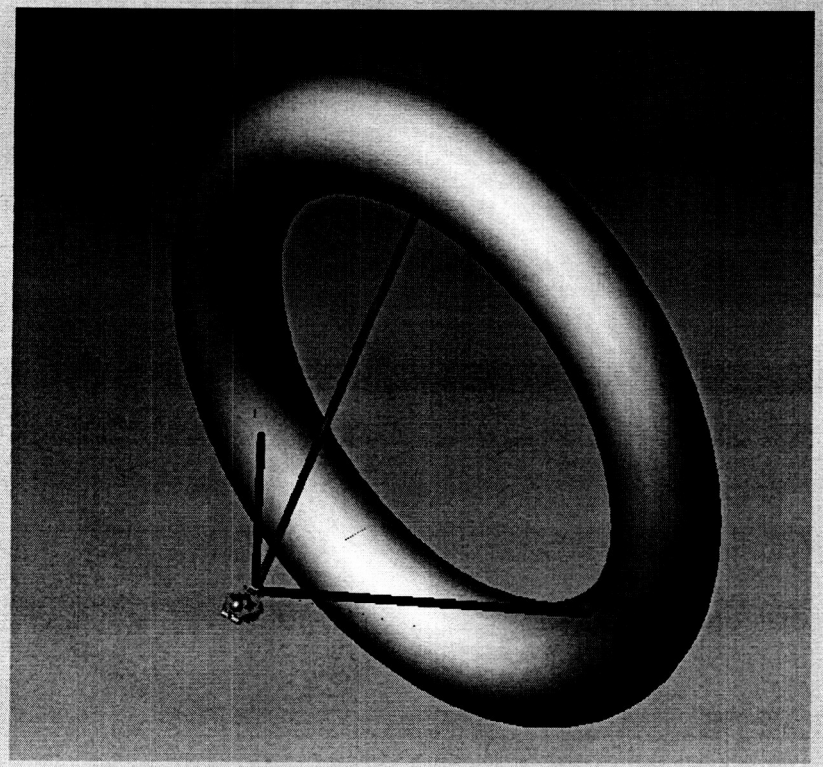

Toroidal Towed Ballute Configuration

- Shape / configuration
- Heating and material limits
- Packing and storage
- Trajectory robustness
- Flow stability
- Aeroelasticity
- Deployment and inflation
- Tether design (for towed ballutes)

HyperPASS

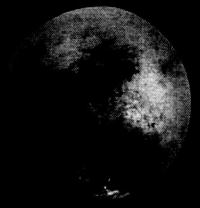

Modeling Assumptions:

- Spherical planetary body
- Inverse-square gravity field
- Rotating atmosphere (with planet)
- Point-mass vehicle representation
- Exponentially interpolated atmosphere
- Constant drag coefficient

Parameter	Orbiter	Ballute/Lander
m	400 kg	100 kg
C_D	1.37	1.37
A	2 m^2	750 m^2
R_n	0.8 m	15.5 m

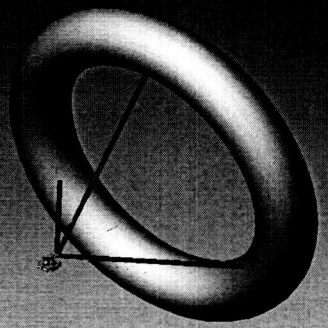

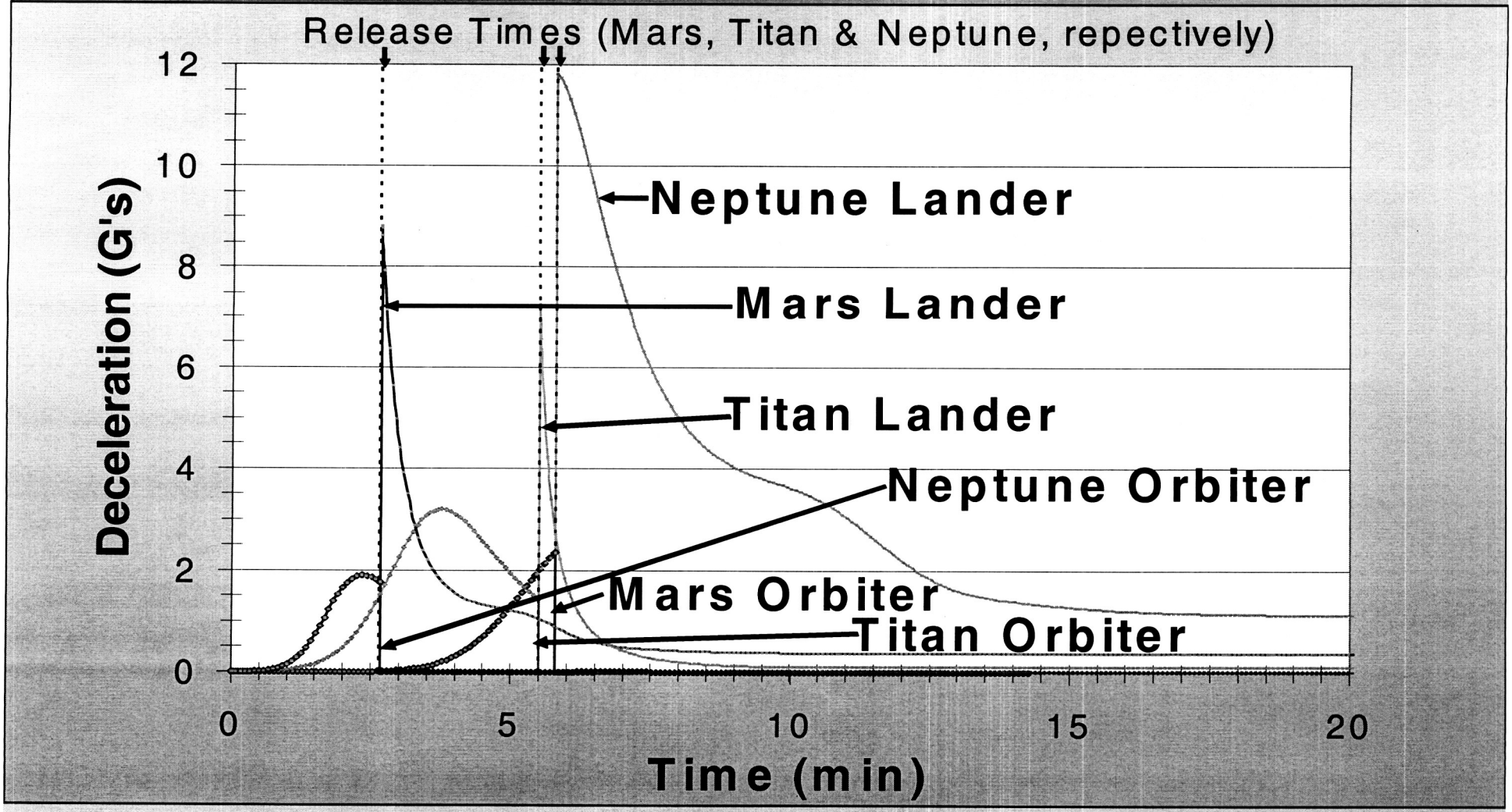
Release Times (Mars, Titan & Neptune, repectively)
Deceleration (G's)
12
10
8
6
4
2
0
0
5
10
15
20
Time (min)
Neptune Lander
Mars Lander
Titan Lander
Neptune Orbiter
Mars Orbiter
Titan Orbiter

Heating Rate Calculations

Goal:

$$Q \leq 3 \ W/cm^2$$

- Stagnation-Point Heating Rate

$$Q_{stag} = \frac{C\rho^{Nstag} v^{Mstag}}{\sqrt{R_n}}$$

- Free Molecular Heating Rate

$$Q_{fm} = \frac{1}{2}\rho v^3$$

Stagnation-Point Heating Rate

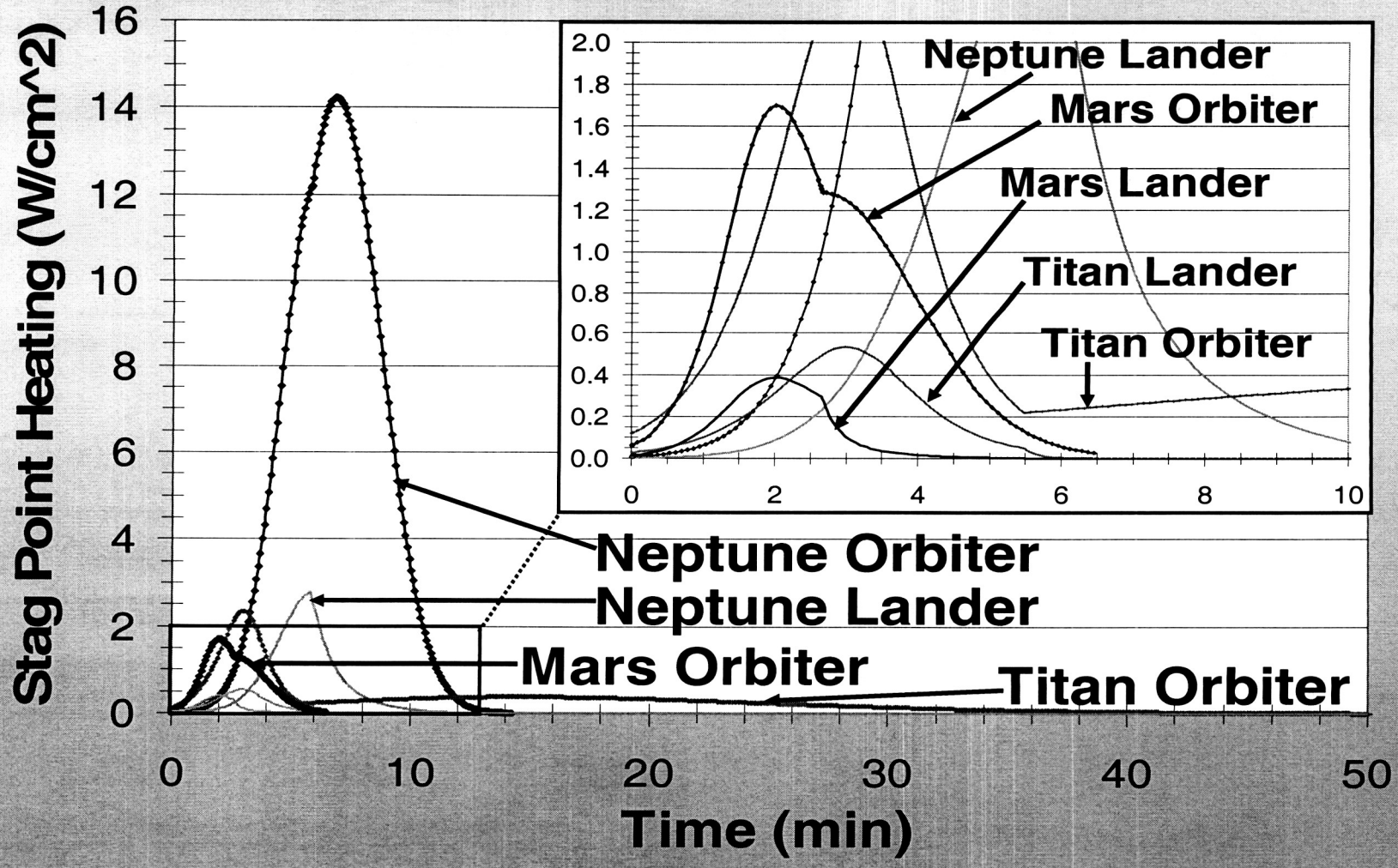

Heating Comparison

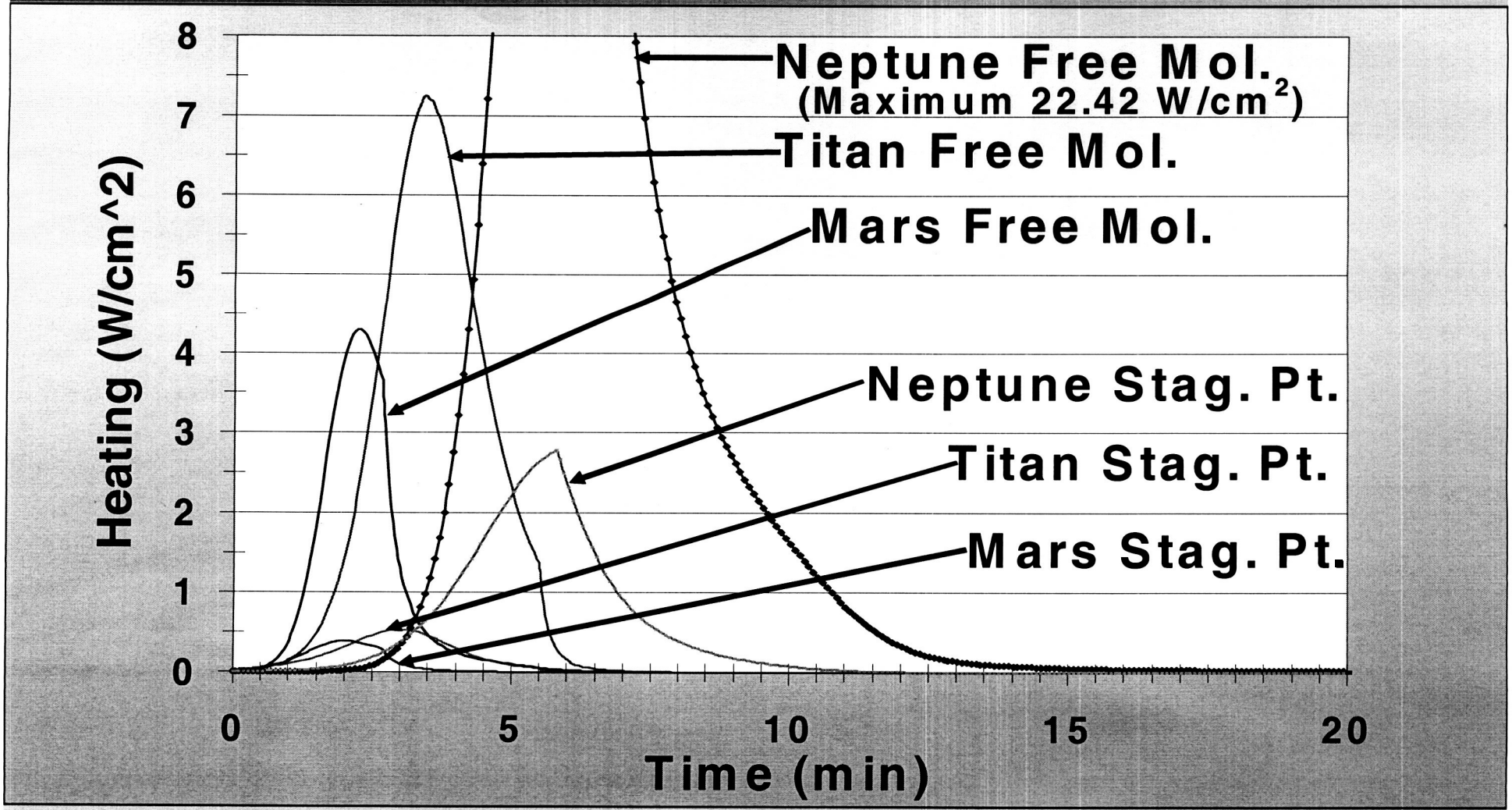

Ballute Area Comparison

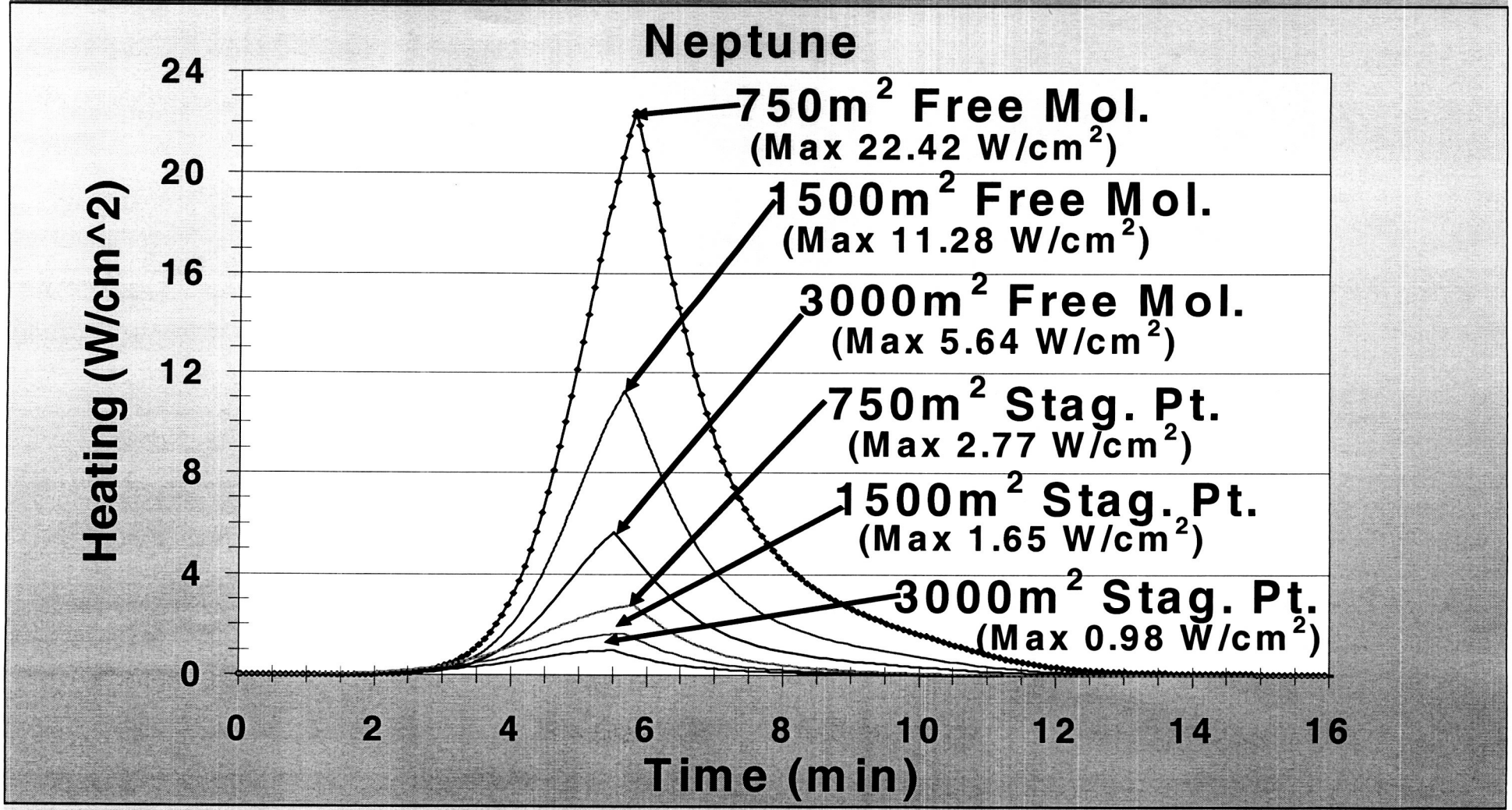

Conclusions: Dual-Use Ballute

- Efficient in delivering payloads to the surface of Titan and Mars
- Applications at Neptune will require a larger area-to-mass ratio
- Offers a significant new technique and tremendous advantages for exploration of the Solar System